

## VARIABLE ULTRAVIOLET ABSORPTION IN THE SPECTRUM OF MR 2251–178<sup>1</sup>

RAJIB GANGULY, JANE C. CHARLTON, AND MICHAEL ERACLEOUS

Department of Astronomy and Astrophysics, 525 Davey Laboratory, Pennsylvania State University,  
 University Park, PA 16802; ganguly@astro.psu.edu, charlton@astro.psu.edu, mce@astro.psu.edu

Received 2001 May 10; accepted 2001 June 11; published 2001 July 9

### ABSTRACT

We present an ultraviolet spectrum of MR 2251–178 taken with *Hubble Space Telescope* (*HST*)/Space Telescope Imaging Spectrograph (STIS) with the G230L grating. The observation is part of a snapshot program of quasars (QSOs) that systematically searches for intrinsic absorption lines through variability. The sample consists of all QSOs observed with the *HST*/Faint Object Spectrograph (FOS) that showed associated narrow absorption lines. The FOS spectrum of MR 2251–178, taken in 1996, showed an associated C IV doublet with a  $\lambda 1548$  equivalent width of  $1.09 \pm 0.09$  Å. It is not detected in the STIS spectrum taken 4 years later, down to a  $3\sigma$  threshold of 0.19 Å. In addition to its other accolades, these observations make MR 2251–178 the very first QSO at low redshift in which the associated absorption is shown to be truly intrinsic. We discuss the implications of this and suggest courses for future study.

*Subject headings:* quasars: absorption lines — quasars: individual (MR 2251–178)

### 1. INTRODUCTION

The identification of quasar-intrinsic narrow absorption lines<sup>2</sup> has increased tremendously over the past 4 years with the advent of high-resolution spectroscopy with large ground-based telescopes. With this increase has come new insights on how to identify these absorbing systems—i.e., on how to separate them from randomly distributed intervening material. Historically, large ensembles of intrinsic absorbers have been identified using statistical arguments, either by demonstrating an excess of absorbers in some redshift path (Foltz et al. 1986; Anderson et al. 1987) or by correlating the velocity distribution (with respect to the QSO emission redshift) of absorbers with QSO properties (Richards et al. 1999). Such surveys have demonstrated that, in high-redshift QSOs, there is an excess of absorbers that lie within  $5000 \text{ km s}^{-1}$  of the QSO emission redshift (termed “associated” absorbers). It is now generally accepted that a large fraction of associated absorbers are indeed intrinsic. However, it is not truly known how large this fraction is. Moreover, Richards et al. (1999) demonstrated that a significant fraction of nonassociated (i.e., high-ejection velocity) absorbers may also be intrinsic.

The two smoking guns, according to Barlow & Sargent (1997), that identify an intrinsic system are (1) the variability of the spectral profiles and/or equivalent widths over time (e.g., Hamann et al. 1995, 1997a; Barlow, Hamann, & Sargent 1997; Hamann, Barlow, & Junkkarinen 1997b; Aldcroft, Bechtold, & Foltz 1997) and (2) the signature of partial coverage (e.g., Barlow & Sargent 1997; Barlow et al. 1997; Hamann et al. 1997c; Ganguly et al. 1999). Thus far, all cases of confirmed QSO-intrinsic NALs are at high redshift, where the resonant UV doublets of metals are shifted into the optical. At low redshift, Ganguly et al. (2001) estimate from statistical excesses that  $\sim 25\%$  of QSOs have intrinsic NALs. As a first step in determining the true fraction of intrinsic NALs and deciphering the dominant cause of variability (if one exists), we have undertaken a *Hubble Space Telescope* (*HST*)/Space Telescope Imaging Spectrograph (STIS) snapshot program to identify in-

trinsic NALs in a sample of QSOs for which associated NALs have been detected in archived *HST*/Faint Object Spectrograph (FOS) spectra. In this effort, we also hope to look for high-ejection velocity absorbers at low redshift and decipher the nature of the variability. We note that, up until now, only six QSOs have been shown to host intrinsic absorption through time variability—all at  $z_{\text{em}} > 1.5$ . Furthermore, all cases of associated, time-variable absorption have been low-luminosity active galactic nuclei (Walter et al. 1990; Shull & Sachs 1993; Maran et al. 1996; Weymann et al. 1997; Crenshaw et al. 2000).

In this Letter, we report the first confirmation at low redshift of an associated NAL that is truly intrinsic to a QSO, MR 2251–178 ( $z_{\text{em}} = 0.066092$ ; Bergeron et al. 1983). The radio-quiet MR 2251–178 is well known for having a highly variable X-ray warm absorber, the first one known (Halpern 1984). Monier et al. (2001) first reported an associated UV absorber and, assuming that the same gas produced the X-ray warm absorption, inferred that the mass-loss rate from the disk and the accretion rate were comparable.

In § 2, we present our *HST*/STIS snapshot of MR 2251–178. In § 3, we show that the associated UV absorption has varied over the past 4 years (thus, verifying its intrinsic nature). In § 4, we discuss the implications of variability on analyses of intrinsic absorption lines and make suggestions for future work on MR 2251–178.

### 2. DATA

The sample for our snapshot program is drawn from QSOs in the *HST*/FOS archive. The sample is restricted to only those QSOs that have been observed with one of the “high”-resolution ( $\sim 230 \text{ km s}^{-1}$ ) FOS gratings (G130H, G190H, and G270H) and for which there is evidence of associated absorption in the form of a C IV  $\lambda\lambda 1548, 1550$ , N V  $\lambda\lambda 1393, 1403$ , O VI  $\lambda\lambda 1032, 1038$ , or Ly $\alpha$  feature. The sample, comprised of 37 QSOs, includes 13 NALQSO candidates from Ganguly et al. (2001), which derived from a subsample of the *HST* Quasar Absorption Line Key Project QSOs, as well as 24 QSOs that were not part of the Key Project. The QSOs from the Key Project (Bahcall et al. 1993, 1996; Schneider et al. 1993; Jannuzi et al. 1998) were obtained from D. Schneider, B. Jannuzi, and S. Kirhakos. The non-Key Project QSOs were reduced and supplied by S. Kirhakos. All

<sup>1</sup> Based on observations with the NASA/ESA *Hubble Space Telescope*, obtained at the Space Telescope Science Institute, which is operated by AURA, Inc., under NASA contract NAS5-26555.

<sup>2</sup> Hereafter, we refer to narrow absorption lines as NALs and to quasars that host truly intrinsic NALs as NALQSOs.

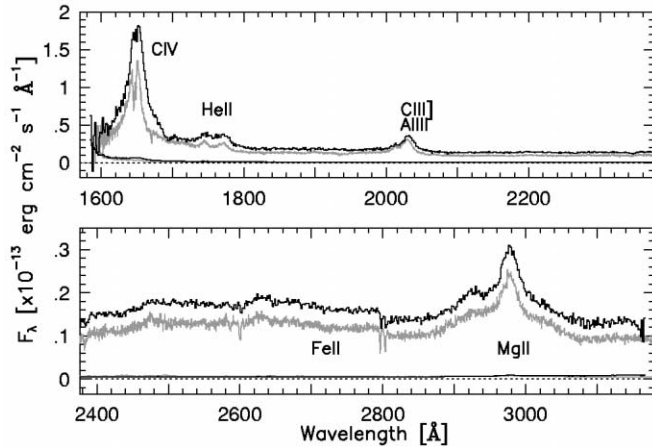


FIG. 1.—STIS-G230L spectrum of MR 2251–178. The two histograms shown are the STIS spectrum (*black histogram*) from 2000 November 5 and the FOS spectrum (*gray histogram*) from 1996 August 2 (Monier et al. 2001). The STIS spectrum covers the range of 1570–3180 Å. The emission lines covered include C IV, He II, C III, Al III, the Fe II complex, and Mg II. Galactic absorption from Fe II and Mg II as well as a hint of the associated C IV absorber are also present.

QSOs were obtained fully reduced with effective continuum<sup>3</sup> fits according to Schneider et al. (1993).

The primary goal of the snapshot program is to detect the variability of associated NALs. To that end, the QSOs are observed using *HST*/STIS with the G230L grating and the  $52'' \times 0.2$  slit. The dispersion of the grating is  $1.58 \text{ Å pixel}^{-1}$ , with two pixels per resolution element. This corresponds to  $300\text{--}600 \text{ km s}^{-1}$  across the spectrum compared with the roughly constant  $230 \text{ km s}^{-1}$  resolution of the FOS spectra. In Figure 1, we show the full spectrum of MR 2251–178 (*black histogram*) resulting from a 500 s exposure taken on 2000 November 5. The signal-to-noise ratio per pixel at  $2376 \text{ Å}$  (the central wavelength) is  $\sim 25$ . The comparison *HST*/FOS spectrum, also shown in Figure 1 (*gray histogram*), was taken on 1996 August 2 with all three  $230 \text{ km s}^{-1}$  resolution gratings (Monier et al. 2001). The relevant portion of the spectrum (taken with the G190H grating) has a signal-to-noise ratio similar to the STIS spectrum. The flux calibration from the reduction pipelines for both the STIS-G230L and FOS-G190H spectra are accurate to within 3%. The wavelength calibration for the FOS-G190H spectrum is accurate to within 0.11 diodes ( $0.2 \text{ Å}$ ), while that of the STIS-G230L spectrum is accurate to within 0.2–0.5 pixels ( $0.3\text{--}0.8 \text{ Å}$ ). A STIS-G140M spectrum, obtained on 1998 February 3 by J. Stocke, spans the wavelength range of  $1194\text{--}1300 \text{ Å}$  (in two separate grating tilts). Although this spectrum covers the associated absorption from Ly $\alpha$  and N V transitions, there is, unfortunately, no overlap with our STIS-G230L spectrum. As a result, no direct comparison can be made with the STIS-G140M spectrum.

### 3. ANALYSIS AND RESULTS

It is apparent by visual inspection of the STIS (Fig. 1) and FOS (Fig. 1 of Monier et al. 2001) spectra that there has been a change in the state of both the emission and associated absorption lines of MR 2251–178. The STIS spectrum has a

<sup>3</sup> The effective continuum is the sum of the continuum and broad emission lines from the QSO. It is the spectrum that is presumably incident on the absorbing gas.

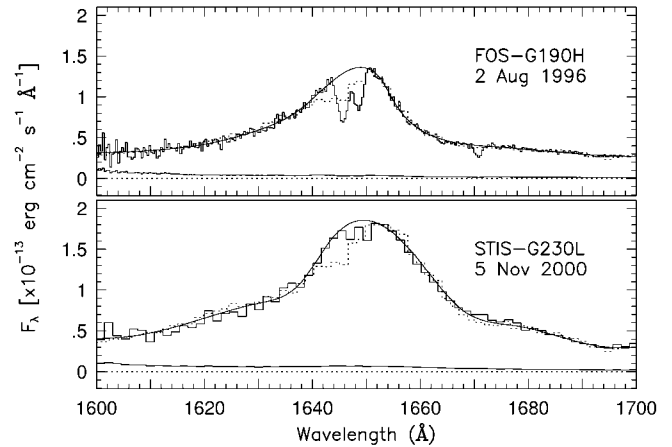


FIG. 2.—Comparison of FOS-G190H and STIS-G230L spectra. In both panels, we show the flux density and error spectrum in the region around the C IV emission line. In the top panel, we show the FOS-G190H spectrum (*solid histogram*), the fit to the effective continuum (*smooth solid spline*), and the expected STIS-G230L spectrum if nothing had varied (*dotted histogram*). In the bottom panel, we show the observed STIS-G230L spectrum (*solid histogram*), the fit to the effective continuum (*smooth solid spline*), and the expected spectrum if no absorber properties had changed (*dotted histogram*). It is clear, to about  $10 \sigma$  confidence, that the associated C IV absorber varied.

generally higher flux, and the associated C IV absorption has apparently disappeared. To examine the magnitude of the variability, we convolved the FOS spectrum with a Gaussian ( $575 \text{ km s}^{-1}$  FWHM) and resampled the result with a  $1.58 \text{ Å pixel}^{-1}$  dispersion to mimic the expected STIS-G230L spectrum around the C IV emission line.

In Figure 2, we show the C IV emission and associated absorption lines from the observed FOS spectrum (*top panel, solid histogram*) and the observed STIS spectrum (*bottom panel, solid histogram*). Overplotted on each are the effective continuum fits (*smooth solid spline*) and the expected STIS spectrum (*dotted histograms*). In the top panel, the expected STIS spectrum reflects what should have been observed if there were no variability in either the C IV emission or associated absorption lines. In the bottom panel, the expected STIS spectrum shows what should have been observed if there were no change in the properties of the associated absorber (i.e., if only the shape of the C IV emission line and the continuum flux changed). With STIS-G230L, the associated C IV absorption is sampled by 7 pixels (3.5 resolution elements) and should have been detected in the observed spectrum. (The Galactic Al II line at  $1670 \text{ Å}$ , which is sampled by less than a pixel in the STIS spectrum, is completely washed out by the instrumental profile, making it indistinguishable from the C IV and He II emission lines.) Furthermore, Monier et al. (2001) measured a C IV  $\lambda 1548$  equivalent width of  $1.09 \pm 0.09 \text{ Å}$  in the FOS spectrum. Using the unresolved feature detection method from Schneider et al. (1993), we find that the absorption line is not formally detected down to a  $3 \sigma$  equivalent width limit of  $0.19 \text{ Å}$ . This is more than a  $10 \sigma$  change in the equivalent width. It is, therefore, clear and robust that there has been variability in the properties of the associated absorber.

### 4. DISCUSSION

#### 4.1. Variability in the UV Spectrum

The change in the state of associated C IV absorption happened sometime in the last 4 years. Although we cannot ac-

curately say on what timescale that variability occurred, it is now safe to say that this is the first clear demonstration of truly intrinsic narrow absorption in a low-redshift QSO. Variability in absorption lines is generally attributed to one of two scenarios. In the first scenario (bulk motion), the absorption gas has an appreciable motion transverse to the line of sight, and the total column density through the gas changes with time. The observational signature is that the equivalent width of all lines due to this gas should change in the same way (i.e., they should all get stronger or all get weaker) with time. In the second scenario (ionization/recombination), the physical state of the absorber changes such that the absorbing gas becomes more or less ionized with time. Observationally, this would mean that the equivalent widths of higher ionization lines and lower ionization lines should change in opposite directions. This assumes, however, that the kinematics of the gas does not change, so that the column densities of the ions drive the changes in the equivalent widths. Unfortunately, the 4 yr separation of the two UV observations and the lack of coverage of relevant species by the STIS-G230L observation (e.g., Ly $\alpha$ , N v  $\lambda\lambda$ 1393, 1403, Si iv  $\lambda\lambda$ 1394, 1403, Si ii  $\lambda$ 1260, and C ii  $\lambda$ 1335) do not allow one to distinguish between these two causes of the variability in the spectrum of MR 2251–178.

Nevertheless, since we know that the variability timescale is less than 4 years, we can provide an upper limit on the distance between the absorbing material and the ionizing sources. If we assume that the cause of variability is the recombination of C iv to C iii and that the temperature of the absorber is about  $T_e = 2 \times 10^5$  K as in UM 675 (Hamann et al. 1995), then the minimum density is  $n_e = 1/t_{\text{rec}}\alpha > 3000 \text{ cm}^{-3}$ , where the recombination coefficient is  $\alpha = 2.8 \times 10^{-12} \text{ cm}^3 \text{ s}^{-1}$  (Arnaud & Rothenflug 1985). This implies a maximum distance of 2.4 kpc, if C iv is the dominant species. This is consistent with the estimate from Monier et al. (2001). While not very restrictive, the distance estimate does rule out a number of candidates for the absorbers, including the intergalactic medium of the host cluster and most of the interstellar medium of the host galaxy. The remaining possible candidates are the material mixed with the broad emission line region, material outside the broad-line region, and outflowing/ejected material.

#### 4.2. Suggestions for Future Work

The next step in understanding the intrinsic absorber in MR 2251–178 is to decipher the cause of variability—bulk motion

or ionization/recombination—and then determine if there is a direct physical relationship between the gas and the X-ray warm absorber. In principle, these issues can be tackled, but they require a regimented observing schedule. To determine efficiently both the underlying cause of variability and the geometry of absorbing gas relative to the central engine, periodic observations at medium-to-high resolution should be obtained of the rest-frame wavelength range of 1200–1600 Å (e.g., with the E140M echelle on STIS). This covers transitions of Si ii, Ly $\alpha$ , N v, C ii, Si iv, and C iv. The frequency of the observations should be less than (or on the order of) once every 2 months. If the QSO and/or absorber properties vary within the course of observations, this schedule should provide the variability timescale. In addition, at high resolution, photoionization modeling of the individual components should constrain the physical conditions of the gas. Furthermore, measurements of the partial coverage fraction are possible (and necessary) with the resolved components. The combination of the partial coverage fraction, the physical conditions of the gas (e.g., the ionization parameter, density), and the variability timescale can constrain the distance from the central engine, the size, and the transverse velocity of the absorbers.

Once the range of conditions in the UV-absorbing gas is known, one can then consider its relationship to the X-ray warm absorber. This, however, is difficult since the X-ray warm absorber is known to vary on short timescales (<1 yr; Halpern 1984). Thus, simultaneous observations of MR 2251–178 in both the UV and the X-ray are required so that inferred relationships are not affected by the changing conditions. In the X-ray, observations can be carried out with either the *Chandra* High-Energy Transmission Grating or the *XMM-Newton* Reflection Grating Spectrometer to cover O vii and O viii. Ultraviolet observations should be carried out with either the *HST*/STIS E140M echelle, which covers a range of ionization states, and/or with the *Far Ultraviolet Spectroscopic Explorer*, which covers the O vi  $\lambda\lambda$ 1032, 1038 doublet and the Lyman series.

Support for this work was provided under grants HST-GO-08681.01-A and STSI AR-08763.01-A. We are grateful to Sofia Kirhakos for providing the uniformly and fully reduced FOS archive with continuum and emission-line fits.

#### REFERENCES

- Aldcroft, T., Bechtold, J., & Foltz, C. 1997, in ASP Conf. Ser. 128, Mass Ejection from Active Galactic Nuclei, ed. N. Arav, I. Shlosman, & R. J. Weymann (San Francisco: ASP), 25
- Anderson, S. F., Weymann, R. J., Foltz, C. B., & Chaffee, F. H. 1987, *AJ*, 94, 278
- Arnaud, M., & Rothenflug, R. 1985, *A&AS*, 60, 425
- Bahcall, J. N., et al. 1993, *ApJS*, 87, 1
- . 1996, *ApJ*, 457, 19
- Barlow, T. A., Hamann, F., & Sargent, W. L. W. 1997, in ASP Conf. Ser. 128, Mass Ejection from Active Galactic Nuclei, ed. N. Arav, I. Shlosman, & R. J. Weymann (San Francisco: ASP), 13
- Barlow, T. A., & Sargent, W. L. W. 1997, *AJ*, 113, 136
- Bergeron, J., Boksenberg, A., Dennefeld, M., & Tarenghi, M. 1983, *MNRAS*, 202, 125
- Crenshaw, D. M., Kraemer, S. B., Hutchings, J. B., Danks, A. C., Gull, T. R., Kaiser, M. E., Nelson, C. H., & Weistrop, D. 2000, *ApJ*, 545, L27
- Foltz, C. B., Weymann, R. J., Peterson, B. P., Sun, L., Malkan, M. A., & Chaffee, F. H. 1986, *ApJ*, 307, 504
- Ganguly, R., Bond, N. A., Charlton, J. C., Eracleous, M., Brandt, W. N., & Churchill, C. W. 2001, *ApJ*, 549, 133
- Ganguly, R., Eracleous, M., Charlton, J. C., & Churchill, C. W. 1999, *AJ*, 117, 2594
- Halpern, J. P. 1984, *ApJ*, 281, 90
- Hamann, F., Barlow, T. A., Beaver, E. A., Burbidge, E. M., Cohen, R. D., Junkkarinen, V., & Lyons, R. 1995, *ApJ*, 443, 606
- Hamann, F., Barlow, T. A., Cohen, R. D., Junkkarinen, V., & Burbidge, E. M. 1997a, in ASP Conf. Ser. 128, Mass Ejection from Active Galactic Nuclei, ed. N. Arav, I. Shlosman, & R. J. Weymann (San Francisco: ASP), 19
- Hamann, F., Barlow, T. A., & Junkkarinen, V. 1997b, *ApJ*, 478, 87
- Hamann, F., Barlow, T. A., Junkkarinen, V., & Burbidge, E. M. 1997c, *ApJ*, 478, 80
- Jannuzi, B. T., et al. 1998, *ApJS*, 118, 1
- Maran, S. P., Crenshaw, D. M., Mushotzky, R. F., Reichert, G. A., Carpenter, K. G., Smith, A. M., Hutchings, J. B., & Weymann, R. J. 1996, *ApJ*, 465, 733
- Monier, E. M., Mathur, S., Wilkes, B., & Elvis, M. 2001, *ApJ*, in press (astro-ph/0102348)
- Richards, G. T., York, D. G., Yanny, B., Kollgaard, R. I., Laurent-Muehleisen, S. A., & vanden Berk, D. E. 1999, *ApJ*, 513, 576
- Schneider, D. P., et al. 1993, *ApJS*, 87, 45

Shull, J. M., & Sachs, E. R. 1993, ApJ, 416, 536

Walter, R., Courvoisier, T. J.-L., Ulrich, M.-H., & Buson, L. M. 1990, A&A, 233, 53

Weymann, R. J., Morris, S. L., Gray, M. E., & Hutchings, J. B. 1997, ApJ, 483, 717